

## COLLECTIVE REORIENTATIONAL MOTION AND NUCLEAR SPIN RELAXATION IN PROTEINS

J. J. PROMPERS, S. F. LIENIN<sup>1</sup>, R. BRÜSCHWEILER  
*Carlson School of Chemistry and Biochemistry, Clark University  
Worcester, MA 01610-1477, USA*

Significant progress in NMR methodology for measuring spin-relaxation data at many different <sup>15</sup>N and <sup>13</sup>C sites in proteins demands new and increasingly sophisticated ways of data interpretation. Recent work of our group concerning the use of anisotropic and reorientational collective motional models for spin-relaxation interpretation is briefly reviewed and a number of important aspects of collective reorientational motional models are discussed at the example of a 11 ns molecular dynamics computer simulation of the protein ubiquitin.

### 1 Introduction

#### 1.1 General

Nuclear magnetic relaxation spectroscopy has emerged as a highly useful method for the experimental characterization of reorientational intramolecular protein dynamics in solution. Motions that can be studied by nuclear spin relaxation lie in the ns and sub-ns range, which includes processes that are of biological relevance. Since the early days of nuclear magnetic resonance (NMR) the interpretation of nuclear spin relaxation parameters, such as  $T_1$ ,  $T_2$ , and NOE (nuclear Overhauser enhancement) [1], has been the subject of ongoing interest. In the pioneering work by Woessner [2] analytical motional models were introduced, such as lattice jump models and diffusion models, containing a small number of motional parameters that were fitted to experimental relaxation data. Since then, alternative philosophies for data interpretation and, in some cases more accurately, data translation have emerged as is depicted in Figure 1. They can be divided into analytical and molecular-force field based descriptions and they include the model-free approach by Lipari and Szabo employing  $S^2$  order parameters [3], the spectral-density mapping by Peng and Wagner [4], and direct back-calculations of relaxation parameters from molecular dynamics (MD) computer simulations as was first demonstrated by Levy, Karplus, and Wolynes [5]. The first two approaches have the goal to avoid overinterpretation of experimental relaxation data, since such data can often be equally well explained by qualitatively different analytical models [3]. The MD approach aims at a physically realistic interpretation of relaxation data using additional knowledge about the system contained in the molecular force field and in the starting conformation of the system obtained by X-ray crystallography or NMR spectroscopy.

---

1. Present address: Paul Scherrer Institut, 5232 Villigen, Switzerland

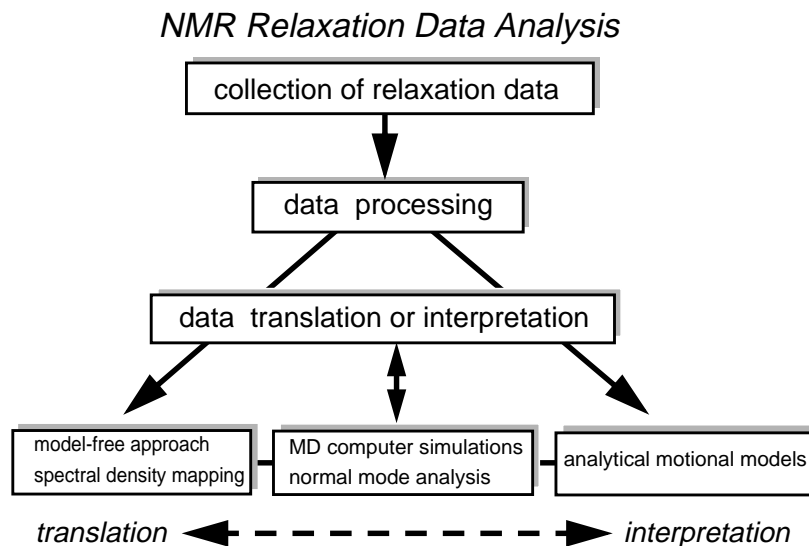


Fig. 1. NMR relaxation data treatment.

### 1.2 Locally anisotropic reorientational motion

Recently, we have developed a hybrid method that uses a MD trajectory as a “dynamical scaffold” from which a realistic analytical model is derived and whose parameters are fitted to experimental data [6]. This approach was applied to internally relatively rigid fragments, such as aromatic side-chain rings [6] and polypeptide backbone peptide planes [7,8]. Heteronuclear relaxation experiments probe reorientational motions that modulate the directions of the principal axes of spin-relaxation active interactions, which are for spin-1/2 nuclei the magnetic dipole-dipole interaction and the chemical-shielding anisotropy (CSA) interaction. If the relaxation-active interactions of spins belonging to the same rigid fragment probe different directions, they allow the detailed characterization of the motional anisotropy of such fragments. For example, in case of  $^{15}\text{N}$  and carbonyl  $^{13}\text{C}'$  spins in the peptide plane, the N-H vector and the CSA principal axes of the  $\text{C}'$  point along different directions allowing the characterization of anisotropic peptide-plane motion in terms of Gaussian axial fluctuations about 3 orthogonal axes (3D GAF model [7,8], see Figure 2). Such a description bears some similarity with anisotropic crystallographic B factors with the important difference that the 3D GAF model exclusively reflects reorientational motions that occur on the sub-ns time-scale range. The backbone peptide-plane dynamics of ubiquitin has been analyzed by using a combination of  $^{15}\text{N}$  and  $^{13}\text{C}'$  spin relaxation data at multiple magnetic fields and MD [8].

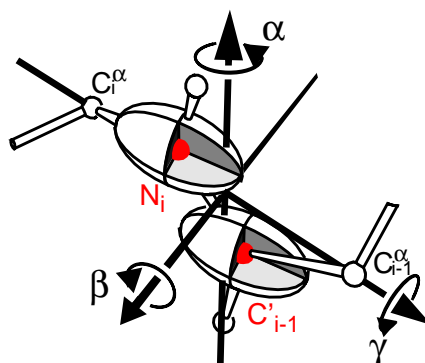


Fig. 2. Visual presentation of the 3D GAF model for the characterization of anisotropic peptide-plane dynamics (adapted from Ref. [7]).

### 1.3 Collective protein dynamics

Besides being locally anisotropic, motions of different protein parts are generally also correlated due to the high density of the protein interior. Because of the short-range nature of spin interactions such correlation effects are inherently difficult to assess from experimental data alone. Normal-mode analysis [9] and quasiharmonic analysis [10], on the other hand, contain abundant information on motional correlations.

We have started to include such information for a comprehensive interpretation of relaxation parameters collected at many different protein sites. There exist a number of different possibilities to do this. In the original approach, the collective relaxation model [11], a normal-mode or quasiharmonic analysis is performed and the amplitudes and directions of the dominant modes are adjusted to fit target relaxation parameters. For the globular protein ubiquitin we have recently found that nuclear spin-relaxation active reorientational motions are to a significant extent “decoupled” from other motions, which suggests the possibility to model such motions in terms of reorientational quasiharmonic modes [12]. They can be described in a reorientational subspace allowing a compact and yet comprehensive description of spin-relaxation active dynamics.

## 2 Collective reorientational protein dynamics

### 2.1 Collective axial fluctuation (CAF) model

The correlations of reorientational motions of principal axes  $\mathbf{e}_k, \mathbf{e}_l$  of unit length, representing, for example, a set of (orthogonal) 3D vectors attached to internally rigid fragments or internuclear directors in the case of dipolar interactions, are characterized in terms of the covariance matrix  $\mathbf{M}$  [12]

$$M_{kl} = \langle (\mathbf{e}_k^T - \langle \mathbf{e}_k^T \rangle) (\mathbf{e}_l - \langle \mathbf{e}_l \rangle) \rangle = \langle \mathbf{e}_k^T \cdot \mathbf{e}_l \rangle - \langle \mathbf{e}_k^T \rangle \langle \mathbf{e}_l \rangle \quad (1)$$

calculated from the scalar products of the vectors  $\mathbf{e}_k, \mathbf{e}_l$ . The angular brackets  $\langle \dots \rangle$  signify an average over the set of structures obtained from a MD trajectory, a Monte Carlo (MC) simulation, or NMR structure determination. The reorientational motions of the  $n$  vectors are spanned by  $n$  orthonormal modes  $\vec{Q}_j$ , which are solutions to the eigenvalue problem

$$\mathbf{M} \vec{Q}_j = \lambda_j \vec{Q}_j, \quad j = 1, \dots, n \quad (2)$$

The  $\vec{Q}_j$  are the reorientational eigenmodes and their amplitudes are reflected in the eigenvalues  $\lambda_j$ . Different aspects of the backbone dynamics of ubiquitin have been analyzed in this way [12].

If correlation effects between different fragments are ignored, Eq. (1) reduces to the 3D GAF model [7,8] with Gaussian axial variances given by

$$\sigma_\alpha^2 = \frac{1}{2} \log \frac{(1 - \lambda_\alpha)}{(1 - \lambda_\beta)(1 - \lambda_\gamma)} \quad (\text{and permutations in } \alpha, \beta, \gamma) \quad (3)$$

where  $\lambda_\alpha, \lambda_\beta, \lambda_\gamma$  are the eigenvalues of the 3x3 blocks along the diagonal of  $\mathbf{M}$ .

### 2.2 Reorientational quasiharmonic dynamics and thermodynamics

The above treatment can be further generalized to establish an effective potential function of reorientational motion, which allows a connection between dynamics and thermodynamics. This is accomplished by defining the  $3n$  dimensional column vector  $\Delta \mathbf{e} = (\mathbf{e}_1 - \langle \mathbf{e}_1 \rangle, \mathbf{e}_2 - \langle \mathbf{e}_2 \rangle, \dots, \mathbf{e}_n - \langle \mathbf{e}_n \rangle)$  which enters the covariance matrix  $\mathbf{P}$  [13]

$$\mathbf{P} = \langle \Delta \mathbf{e} \cdot \Delta \mathbf{e}^T \rangle \quad (4)$$

Matrix  $\mathbf{M}$  of Eq. (1) is retrieved by trace formation over all 3x3 sub-matrices of matrix  $\mathbf{P}$ . The potential energy function associated with relaxation-active reorienta-

tional displacement  $\Delta \mathbf{e}$  is defined by

$$V_{active}(\Delta \mathbf{e}) = \frac{kT}{2} \Delta \mathbf{e}^T \mathbf{P}^{-1} \Delta \mathbf{e} \quad (5)$$

$V_{active}(\Delta \mathbf{e})$  is temperature dependent which is a common property of quasiharmonic potential energy functions [10]. From  $V_{active}$  the associated reorientational partition function  $Z_{active}$  can be determined from which reorientational thermodynamic quantities, such as free energy and entropy, can be derived [13].

### 2.3 MD trajectories used for analysis

Reorientational quasiharmonic modes can be extracted from a MD trajectory. For this purpose, a 11 ns MD simulation of native ubiquitin in aqueous solution has been performed using the program CHARMM [14,15] (for details see Ref. [8]). First, matrix  $\mathbf{P}$  of Eq. (4) was computed from 1000 snapshots taken from the interval between 1 and 2 ns (increment of 1 ps). A set of 3 orthogonal vectors was extracted from each snapshot for each of the  $N = 72$  (non-proline) peptide planes leading to  $n = 3 \times 72 = 216$  vectors  $\mathbf{e}_k$ . For comparison, two more matrices  $\mathbf{P}'$ ,  $\mathbf{P}''$  were constructed from 1000 snapshots each taken between 1 and 6 ns and 1 and 11 ns with an increment of 5 ps and 10 ps, respectively. All three matrices  $\mathbf{P}$ ,  $\mathbf{P}'$ ,  $\mathbf{P}''$ , which have dimension  $3n = 648$ , were diagonalized leading to sets of eigenmodes and eigenvalues  $\{\vec{Q}_j, \lambda_j\}$ ,  $\{\vec{Q}'_j, \lambda'_j\}$ ,  $\{\vec{Q}''_j, \lambda''_j\}$  ( $j = 1, \dots, 648$ ), respectively. All eigenmodes were normalized ( $\vec{Q}_j^T \cdot \vec{Q}_j = 1$ ) and sorted according to increasing eigenvalues. The three parts of the MD trajectory are analyzed in the following sections.

### 2.4 Mode collectivity measures

The presence of motional correlations between backbone fragments is manifested in form of eigenmodes that simultaneously affect more than one fragment. A mode is highly collective if its components are spread out over many different fragments, while it is localized if it affects a single fragment or a few fragments only. A quantitative measure of collectivity is the *mode collectivity index*, or simply the *collectivity*,  $\kappa_j$  [16]. We describe here different versions of such a measure and compare the results.

Each eigenvector  $\vec{Q}_j$  can be cast into  $N = 72$  9-dimensional components  $\vec{q}_{j,k} = (Q_{j,9k-8}, \dots, Q_{j,9k})$  ( $k = 1, \dots, N$ ). The  $\vec{q}_{j,k}$  can be translated into squared amplitudes or “populations”  $p_{j,k} = |\vec{q}_{j,k}|^\gamma / \sum_{m=1}^N |\vec{q}_{j,m}|^\gamma$  which obey the normalization condition  $\sum_{k=1}^N p_{j,k} = 1$ . The collectivity of mode  $j$  is then defined by [16]

$$\kappa_j = \frac{1}{N} \exp \left\{ - \sum_{k=1}^N p_{j,k} \log p_{j,k} \right\} \quad (6)$$

where  $\kappa_j$  is a number between  $1/N$  and 1 given by the ratio between the effective number of fragments that are significantly affected by the  $j$ th mode and the total number of fragments. A low  $\kappa$  reflects local motion, while a high  $\kappa$  reflects a substantial degree of collectivity. The exponent  $\gamma$  allows one to adjust the influence of larger *versus* smaller components  $p_{j,k}$ . In previous work [12,16]  $\gamma$  was set to 2. Here we investigate the results for  $\gamma = 0.5, 1.0, 2.0, 4.0$  for the quasiharmonic reorientational modes of matrix  $\mathbf{P}$  as shown in Figure 3. The magnitude of  $\gamma$  specifies the meaning of “significantly affected”: the smaller  $\gamma$  the larger becomes the relative weight of those fragments that are only slightly affected by a given mode. On the other hand, if  $\gamma$  is large only fragments are taken into account that are strongly affected by a certain mode. While the choice for  $\gamma$  is ultimately subjective,  $\gamma = 2$  represents in our experience a reasonable choice (see also Fig. 1 of Ref. 12).

Figure 3 shows that the  $\kappa$  vs.  $\lambda$  dependence is doubly peaked. Since the orientation of each peptide plane is defined by 3 orthogonal, rigidly attached unit vectors  $\mathbf{e}_k$  (tripod), the effective number of degrees of freedom is  $3N$  with the associated quasiharmonic modes falling on the right peak of the  $\kappa$  distribution (large  $\lambda$  region). The left peak originates from higher order correlation effects in the MD trajectory with modes that would result in internal deformations of the local tripods. They are not further discussed here.

### 2.5 Mode overlaps of different parts of the trajectory

It is useful to compare the reorientational modes of the three sections of the MD trajectory. One possibility consists of the  $\kappa$  vs.  $\lambda$  plots for all three MD sections as shown in Figure 4a. The ranges for  $\kappa$  and  $\lambda$  are very close for all three MD sections

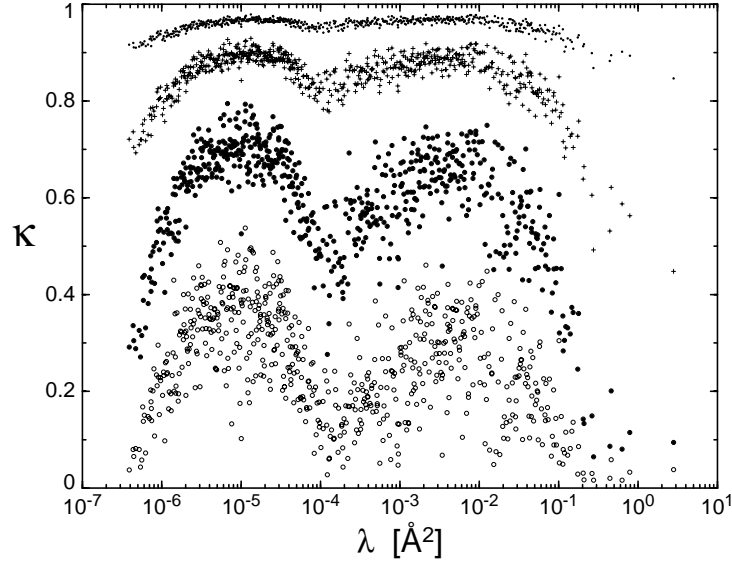


Fig. 3. Mode collectivities  $\kappa$  vs. eigenvalues  $\lambda$  determined from a 1 - 2 ns MD trajectory of ubiquitin (matrix  $\mathbf{P}$ ) according to Eq. (6) for different values of  $\gamma$ :  $\gamma = 4$  (open circles),  $\gamma = 2$  (closed circles),  $\gamma = 1$  ('+' symbols),  $\gamma = 0.5$  (small dots).

as are the  $\kappa$  vs.  $\lambda$  scatter plots. A measure of the overlap  $O_{pp'}^{(r)}$  of the subspaces spanned by the  $r$  eigenvectors  $\{\vec{Q}_j\}$  and  $\{\vec{Q}'_j\}$  with largest eigenvalues is given by the trace norm

$$O_{pp'}^{(r)} = \frac{1}{r} \text{Tr} \left\{ \left( \sum_{j=1}^r \vec{Q}_j \cdot \vec{Q}_j^T \right) \cdot \left( \sum_{j=1}^r \vec{Q}'_j \cdot \vec{Q}'_j^T \right) \right\} \quad (7)$$

Index  $r$  varies between 1 and  $9N$ . The full spaces do completely overlap, therefore  $O_{pp'}^{(9N)} = 1$ . In Figure 4b, the cumulative overlaps  $O_{pp'}^{(r)}$ ,  $O_{pp''}^{(r)}$ ,  $O_{p'p''}^{(r)}$  are plotted as a function of the number of modes  $r$ . The steep increase at the beginning indicates that the subspaces spanned by the large amplitude modes of the three MD sections have a strong overlap. Hence, all three sections sample similar types of protein dynamics with the 5 ns and 10 ns sections behaving most similar and the 1 ns and 10 ns sections exhibiting the largest difference. In addition, the mode overlaps are shown as a reference for two symmetric random matrices of dimension 216 (with elements randomly varying between -1 and 1). They show a linear increase of the overlap, which is very different from the MD cases.

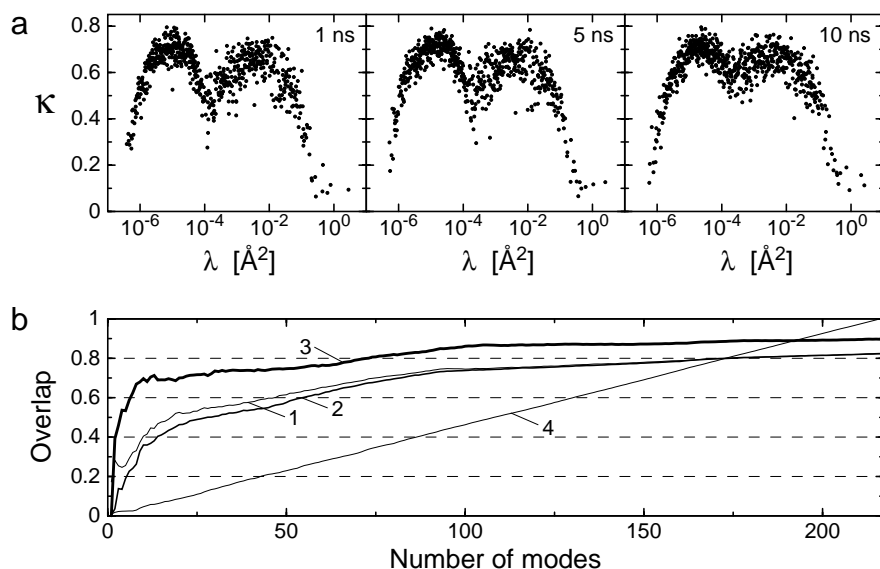


Fig. 4. (a) Mode collectivities  $\kappa$  vs. eigenvalues  $\lambda$  for three sections of a MD trajectory of ubiquitin of 1 ns, 5 ns, and 10 ns length, respectively. (b) Cumulative mode overlaps of the quasiharmonic reorientational modes of the three MD sections of ubiquitin (calculated from matrices  $\mathbf{P}$ ,  $\mathbf{P}'$ ,  $\mathbf{P}''$ ) calculated according to Eq. (7). Line 1 compares the 1 ns and 5 ns trajectories, line 2 compares the 1 ns and 10 ns trajectories, and line 3 compares the 5 ns and 10 ns trajectories. Line 4 compares two symmetric random matrices (with elements randomly varying between -1 and 1).

### 2.6 Number of dominant modes per residue

The relative number of different modes that reorient a given fragment  $k$  is obtained using a measure that is related to the collectivity of Eq. (6)

$$\eta_k = \frac{1}{9N} \exp \left\{ - \sum_{j=1}^{9N} \frac{1}{9} |\hat{q}_{j,k}|^2 \log \left( \frac{1}{9} |\hat{q}_{j,k}|^2 \right) \right\} \quad (8)$$

where  $\eta_k \in [1/(9N), 1]$ . A low  $\eta_k$  value reflects an effective involvement of a small number of modes in the reorientational dynamics of fragment  $k$ , while a high  $\eta_k$  value indicates that a large number of modes contribute significantly. In Figure 5  $\eta_k$  is plotted as a function of the peptide-plane number for the 1 - 2 ns MD section.  $\eta_k$  is for all peptide bonds smaller than 0.7. The backbone parts with large-ampli-

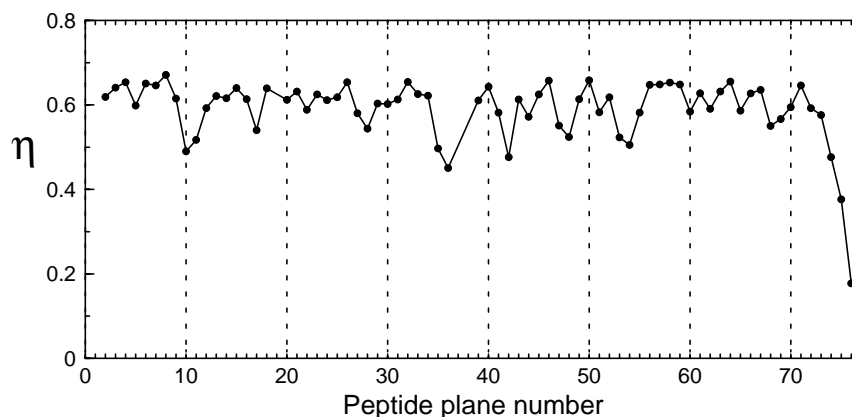


Fig. 5. Number of dominant modes per residue  $\eta$  determined from a 1 - 2 ns MD trajectory of ubiquitin (matrix  $P$ ) according to Eq. (8).

tude motions experience on average a smaller number of modes than the more rigid parts. On the other hand, more rigid parts are not necessarily affected by a larger number of modes.

Applications of these methods to protein side-chain dynamics and to partially folded protein systems to learn more about protein flexibility from our NMR data is currently under way in our group.

### Acknowledgments

J.J.P. is a recipient of a Human Frontier Science Program postdoctoral fellowship. This work was supported by NSF Grant MCB-9904875.

### References

- 1 A. Abragam, *Principles of Nuclear Magnetism* (Clarendon, Oxford, 1961).
- 2 D.E. Woessner, *J. Chem. Phys.* **36**, 1 (1962).
- 3 G. Lipari and A. Szabo, *J. Am. Chem. Soc.* **104**, 4546 & 4559 (1982).
- 4 J. Peng and G. Wagner, *Biochemistry* **31**, 8571 (1992).
- 5 R. M. Levy, M. Karplus, and P. G. Wolynes, *J. Am. Chem. Soc.* **103**, 5998 (1981)

- 6 T. Bremi, R. Brüschweiler, and R. R. Ernst, *J. Am. Chem. Soc.* **104**, 4546 (1982).
- 7 T. Bremi and R. Brüschweiler, *J. Am. Chem. Soc.* **119**, 6672 (1997).
- 8 S. F. Lienin, T. Bremi, B. Brutscher, R. Brüschweiler, and R. R. Ernst, *J. Am. Chem. Soc.* **120**, 9870 (1998).
- 9 T. Noguti and N. Gō, *J. Phys. Soc. Jpn.* **52**, 3283 (1983); B. Brooks and M. Karplus, *Proc. Natl. Acad. Sci. U.S.A.* **80**, 6571 (1983); M. Levitt, C. Sander, and P. S. Stern, *J. Mol. Biol.* **181**, 423 (1985).
- 10 R. M. Levy, M. Karplus, J. Kushick, and D. Perahia, *Macromolecules* **17**, 1370 (1984).
- 11 R. Brüschweiler and D. A. Case, *Phys. Rev. Lett.* **72**, 940 (1994).
- 12 S. F. Lienin and R. Brüschweiler, *Phys. Rev. Lett.* **84**, 5439 (2000).
- 13 J. J. Prompers and R. Brüschweiler, *J. Phys. Chem.* (in press).
- 14 R. B. Brooks, R. E. Bruccoleri, B. D. Olafson, D. J. States, S. Swaminathan, and M. Karplus, *J. Comput. Chem.* **4**, 187 (1993).
- 15 A. D. MacKerell Jr. et al., *J. Phys. Chem. B* **102**, 3586 (1998).
- 16 R. Brüschweiler, *J. Chem. Phys.* **102**, 3396 (1995).